LA-UR-79-1474

CONF-790509--4

MASTER

TITLE:

BROADLY TUNABLE PICOSECOND IR SOURCE

AUTHOR(S):

A. J. CAMPILLO, R. C. HYER, S. L. SHAPIRO

SUBMITTED TO:

PROCEEDINGS OF THE CONFERENCE ON OPTICS '79

University of California

DISTRIBUTION OF THIS DOCUMENT IS UNLIMITED

LOS ALAMOS SCIENTIFIC LABORATORY
Post Office Box 1663 Los Alamos, New Mexico 87545
An Affirmative Action/Equal Opportunity Employer

Form No. 836 R3
St. No. 2629

UNITED STATES

BROADLY TUNABLE PICOSECOND IR SOURCE*

A. J. Campillo+, R. C. Hyer and S. L. Shapiro
University of California, Los Alamos Scientific Laboratory
Los Alamos, NM 87545

ABSTRACT

We report a completely grating tuned (1.9 to 2.4 μm) picosecond traveling wave IR generator capable of controlled spectral bandwidth operation down to the Fourier Transform limit. Subsequent down conversion in CdSe extends tuning to 10 to 20 μm.

I. Introduction

We report a picosecond traveling wave parametric device capable of controlled spectral bandwidth down to the Fourier transform limit, tunable over the range 1.33 - 3.6 μm. This device has the practical advantage that from 1.9 to 2.4 μm, it can be tuned simply by rotating a grating and is extremely stable. We also report the generation of tunable 10-20 μm picosecond radiation by subsequent difference frequency mixing. Use of CdSe is convenient for this purpose due to the fortuitous coincidence of a turning point in the down conversion tuning curve near 16 μm and the relatively large angular tolerance for phasematching, allowing a wide band of frequencies to be accessed without the need for crystal rotation. Thus, the operating wavelength in the 16 μm region and the bandwidth of the entire system are again completely controlled by the grating.

Picosecond pulses have been generated in the IR (1.3-3.6 μm) in the past using 1.06 μm pumped lithium niobate optical parametric devices in both the traveling wave mode[1] and the resonant cavity configuration[2]. The simpler single pass traveling wave devices[3-7] are practical because of the extremely high electric fields and resultant high gains ($> e^{30}$) available with ultrashort pulses. These short pulses allow useful operation below the damage threshold of $LiNbO_3$.

There are several disadvantages associated with previous devices that our scheme successfully overcomes. The first disadvantage is that the spectral bandwidths of earlier devices were primarily determined by phase matching conditions in the nonlinear crystal. Fourier transform limited pulses are normally generated only when the device is tuned far from degeneracy, thereby severely restricting the useful operating range. For example, the spectral bandwidth over the 1.7-2.8 μm region was found to be too broad ($>$100 cm^{-1}) to be useful in many applications[1]. However, operation near the degenerate point is desirable because subsequent mixing of the signal and idler in CdSe would generate radiation from 10-20 μm. In this wavelength region a picosecond source could interrogate infrared active modes of polyatomic molecules in various media, including gaseous. Prior to this paper, such a picosecond IR source had not been reported in the literature.

Another drawback of the usual parametric traveling wave scheme is that nonlinear interactions also allow noncollinear components to experience high gain resulting in a highly divergent beam. The spatial properties can be improved, however, by positioning a second crystal further downstream where the pump beam overlaps and amplifies only collinear components[7]. The resultant beam has desirable beam divergence properties ($<$ 3 mrad) but may still be spectrally broad. Furthermore, when using several crystals, the iterative tuning process is tedious, and the entire assembly is unstable to mechanical and thermal fluctuations.

Our scheme successfully bypasses these difficulties by first generating a broadband (1.9-2.4 μm) picosecond continuum in lithium niobate and then isolating and injecting a specific spectral/spatial component into a second broadband parametric amplifier. The success of our scheme depends upon both the extreme broadband behavior of picosecond traveling wave OPAs and the ability of a simple grating arrangement to achieve adequate spatial/spectral separation.

2. SYSTEM OVERVIEW

Our experimental eonfiguration is depicted schematically in Fig. 1. A repetitively flashlamp pumped (10 Hz) mode-locked Nd:YAG laser emits a train of 40 ps duration pulses on each flashlamp cycle. A single pulse is selected from the train by a cross polarizer Pockels cell arrangement, is amplified in two 1/4 in diameter Nd:YAG amplifiers, and is split along two paths. One beam is directed through a 4.5 cm long, $\theta = 45°$ cut lithium niobate crystal acting as a traveling wave parametric oscillator via the type I phase matched process ($\nu_p^e \rightarrow \nu_s^o + \nu_i^o$). Here ν_p^e represents the frequency of the 1.064 μm extraordinary pump, and ν_s^o and ν_i^o represent the ordinary signal and idler frequencies, respectively. Near degeneracy ($\nu_i \sim \nu_s$) the gain bandwidth of $LiNbO_3$ is extremely broad. This point is discussed in section 3. Thus, spontaneous parametric scattered light within this band is highly amplified and emitted at various angles due to the high gains also experienced by noncollinear components. With a pump energy of 6-8 mJ in a beam waist, w_0, of 2 mm, a sum total of 200 μJ of signal and idler was observed with collection over all angles. At high pump energies there was a strong saturation in output energy which could not be explained by pump depletion. Recent work[8] by our group has demonstrated that the conversion is limited by the nonlinear refractive index, n_2, acting through the term n_2E^2. At high pump intensities (~ 6 GW/cm^2) the phase front near the center of the pump beam is retarded by π radians with respect to the polarization term at ν_p produced by the freely traveling signal and idler beams as they pass through the 4.5 cm long crystal. This phase change effectively mismatches the process and causes energy to flow back into the pump field.

The spectral content of the collinear and nearly collinear (< 4 mrad) components of the emission from the traveling wave oscillator was found experimentally to extend nearly uniformly from 1.92 - 2.38 μm. Outside this range there was a sharp drop off. The spectral shape was determined by aperturing the output and analyzing the spectra of the nearly collinear components using a 1 meter Spex monochromator and a PbS detector.

The emission from the first crystal is diffracted by a grating (600 lines/mm), and the desired spectral and spatial component injected into a second nearly degenerate 2 cm long $LiNbO_3$ amplifier located in the second pump beam line. Collinear components at a specified ν_s are directed into the parametric amplifier by rotating the grating. Overlap of these components with the pump allows preferential amplification. Although it is not immediately obvious, other noncollinear components (at somewhat different ν_s) from the first crystal and striking the grating at different loci than the collinear and yet diffracting to overlap the pump in the second amplifier, apparently experience relatively little gain. Factors contributing to gain reduction for these components include incomplete spatial overlap with the pump, phase mismatch, and temporal noncoincidence with the pump. In any event, placing an aperture after the grating would assure that only the desired spatial/spectral component would be subsequently amplified.

As the injected component is amplified, the corresponding idler is regenerated. Both signal and idler were each typically about 0.5 mJ in energy and 10-15 ps in duration when a pump of 10 mJ was used. The wavelength and spectral purity were totally controlled by the grating. Figure 2 shows the observed output wavelength of the $LiNbO_3$ amplifier versus grating angle. The solid line is that predicted by the grating formula

$$d\,(\sin\alpha + \sin\beta) = m\lambda \qquad (1)$$

where α and β are the angles of the incident and diffracted beams, respectively, defined with respect to the grating normal, d is the spacing of the grating and m is the grating order. In our experiment $\beta - \alpha = 32.5°$ and $m = 1$. Good agreement between theory and observation indicates that the grating alone is controlling the operating wavelength.

The grating also controls the observed bandwidth. In one study both the signal and idler were observed to be 15 cm^{-1} in width (FWHM) when the crystal was placed 1.18 m from the grating and when a pump beam waist, w_0, of 2 mm was used. This agrees well with the 16 cm^{-1} bandwidth calculated from the grating dispersion (6.67 cm^{-1}/mrad) multiplied by the effective angle subtended by the pump in the crystal. By moving the crystal further from the grating a Fourier transform limited pulse of 2 cm^{-1} could in principle be obtained. Based upon gain calculations we estimate the 2 μm pulses have a duration of 10-15 ps.

Our arrangement is extremely easy to align once temporal coincidence is achieved. Should the beam wander due to mechanical changes, another spectral/spatial component moves into alignment at a slightly shifted wavelength. In general, we have found the entire assembly (i.e., crystals, grating) to be highly stable and reliable. This is in marked contrast to picosecond OPOs operated in the resonant cavity configuration[9].

Signal and idler are subsequently mixed in a CdSe crystal to generate tunable IR pulses at the difference frequencies. This is achieved via a Type IIa phase matched process[10], $\nu_s^o + \nu_i^e \rightarrow \nu_{IR}^o$. For a 1 cm long crystal with $\theta = 64.35°$, a band from 540 - 675 cm^{-1} (FWHM) is phasematched. This allows a wide range of frequencies around 16 μm to be generated without the need for crystal rotation. Again, the tuning and bandwidth in the 14.8 - 18.5 μm region is controlled by the grating. Outside this range it is necessary to rotate the CdSe crystal. In preliminary experiments we have observed 2 μJ of tunable radiation over the 14.8 - 18.5 μm region. Though somewhat less than expected, signal and idler energies were limited by passage through nonoptimized filters. These filters were required to prevent optical damage to the CdSe crystal by the 1.064 μm beam and they can be replaced.

3. BROADBAND BEHAVIOR OF NEARLY DEGENERATE OPA

In Section 2 we reported bandwidths for the nearly degenerate 4.5 cm long traveling wave OPO and 2 cm long OPA to be approximately 1000 and 900 cm^{-1}, respectively. Although a broad band is expected for a nearly degenerate picosecond traveling wave OPO or OPA, it had not been recognized that the spectral width would be so extreme. The origins of this broadband behavior can, however, be accounted for adequately by theory, and we summarize the physical mechanisms responsible for this phenomenon.

For predicting the bandwidth the usual method would be to calculate the small signal gain involving the term $\mathrm{sinc}^2(\Delta k\ell/2)$ where $\Delta k = k_p - k_s - k_i$ is the phase mismatch. This expression leads to a FWHM bandwidth given by $(\Delta k)_{BW} \simeq 2\pi/\ell$, where ℓ is the crystal length. Thus, the bandwidth is simply $(\Delta\nu)_{BW} \simeq 1/[\ell(n_i - n_s)]$, where n_i and n_s are the indices of refraction of the idler and signal, respectively. As ν_i approaches ν_s (degeneracy), $n_i - n_s$ approaches zero and $\Delta\nu_{BW}$ becomes very large. Near degeneracy, $(\Delta\nu)_{BW}$ is usually given in the literature[11] by

$$(\Delta\nu)_{BW} = \frac{1}{\ell\left(n_i - n_s + \frac{\partial n_i}{\partial \nu}\nu_i - \frac{\partial n_s}{\partial \nu}\nu_s\right)} \qquad (2)$$

However, three additional factors contribute to the observed bandwidth: 1) operation near degeneracy (slightly off); 2) nearly collinear phase matched components; and 3) parametric gain broadening. The first factor leads to a greater bandwidth than predicted by Eq. 2 slightly off the degenerate point. Figure 3 shows the calculated gain for a 4.5 cm $LiNbO_3$ crystal operating near degeneracy. Sellmeier equations obtained from Ref. 12 were used in these computations. Curve A is computed at the precise theoretical degenerate point, $\theta = 44.672°$. Curves B and C are computed for $44.68°$ and $44.69°$, respectively. Curve B demonstrates an effective bandwidth of approximately 400 cm^{-1} (FWHM) which is greater than that predicted by Eq. 2.

The curves in Fig. 3 were calculated assuming purely collinear interactions. Near degeneracy, however, a second factor, noncollinear component gains, becomes important. In Fig. 4, calculated gains for slightly noncollinear interactions at degeneracy are shown. Here α is the angle between $\vec{k}_s$ and $\vec{k}_p$. In these calculations $\vec{k}_i$ is directed so as to minimize the total $\vec{\Delta k}$. From Fig. 4 we see that even for small α (less than 4.5 mrad), such as that normally encountered in typical beams, the wavelength of maximum gain is shifted significantly. In practice, then, the measured small signal bandwidth will be a superposition of curves as shown in Fig. 4 and thus represents a substantial broadening contribution.

However, a third factor, gain broadening, is the predominant mechanism leading to wide spectral output, though the preceding two mechanisms, as we have seen, do contribute and are in no way insubstantial. The gains encountered in picosecond traveling wave OPAs are extremely high. An expression for the gain of an OPA is[11]

$$G = \Gamma^2 \ell^2 \frac{\sinh^2 \left[\left(\Gamma^2 - \frac{\Delta k^2}{4} \right)^{1/2} \ell \right]}{\left(\Gamma^2 - \frac{\Delta k^2}{4} \right) \ell^2} \tag{3}$$

where $\Gamma^2 \ell^2 = 2\omega_s \omega_i \eta_s \eta_i \eta_p |d'| \ell^2 P_p / A$ and η are the plane wave impedances (377/n). The notation of Ref. 11 is used here. For small values of Γ the above expression reduces to the usual $\Gamma^2\ell^2 \operatorname{sinc}^2 \frac{\Delta k \ell}{2}$. However, Byer[13] has pointed out that significant broadening occurs as $\Gamma^2 \ell^2$ becomes large. This effect is illustrated for the case of our 4.5 cm long traveling wave OPA in Fig. 5. At $\theta = 44.69°$ for the case $\Gamma = 6$, which corresponds to 6 mJ of pump in a 40 ps pulse with a beam waist, w_0, of 2 mm, the spectral output is significantly broader ($\Delta\nu_{BW} \sim 800$ cm^{-1}) than in the small signal gain case.

This gain factor plus the aforementioned superposition of noncollinear components of 4 mrad and less can account for the observed ~1000 cm^{-1} bandwidth of our traveling wave OPO.

A similar calculated distribution for our 2 cm long OPA operated at a pump energy of 10 mJ is compared in Fig. 6 with the measured relative gains as a function of wavelength. Because the exact cut of our crystal was not known to better than 0.1°, the data of Fig. 6 was obtained by rotating the crystal until the observed peak in the gain curve appeared near 5000 cm^{-1}. At that angular setting the relative gain of the amplifier was obtained by rotating the grating so as to vary the wavelength of the input signal. Agreement between experiment and theory was excellent.

4. CONCLUSION

Prior to this paper the only existent picosecond source in the 10 to 20 μm range was the 10.6 μm CO_2 laser. We have demonstrated successful operation of a broadly tunable picosecond IR source which is continuously tunable and which permits the extension of the picosecond spectroscopy field over a wide region in the infrared. The bandwidth and operating wavelength are completely controlled by the use of a grating. The overall setup is simple, stable and reliable.

We have explained the extreme broadband behavior of picosecond traveling wave OPAs by obtaining good agreement between expeeriment and theory. We expect the high powers and picosecond temporal resolution to prove useful for multiphoton studies.

ACKNOWLEDGEMENTS

We thank R. Fleming, C. Milich, M. Sorem and D. Taylor for helpful discussions and K. R. Winn for expert technical assistance. We thank J. Birely for his support and encouragement.

* Supported by the US Dept. of Energy

† Present address: Brookhaven National Laboratory, Dept. of Energy and Environment, Upton, NY, 11973

REFERENCES

1. Laubereau, A., L. Greiter and W. Kaiser, Appl. Phys. Lett. 25, 87(1974).
2. Tanaka, Y., T. Kushida and S. Shionoya, Opt. Comm. 25, 273(1978).
3. Akhmanov, A. G., S. A. Akhmanov, R. V. Khokhlov, A. I. Kovrigin, A. S. Piskarskas and A. P. Sukhorukov, IEEE J. Quantum Electron. QE-4, 328(1968).
4. Burneika, K., M. Ignatavicius, V. Kabelka, A. Piskarskas and A. Stabinis, IEEE J. Quantum Electron QE-8, 511 (1972).
5. Rabson, T. A., H. J. Ruiz, P. L. Shah and F. K. Tittel, Appl. Phys. Lett. 21, 129 (1972).
6. Danelyus, R., G. Dikchyus, V. Kabelka, A. Piskarskas, A. Stabinis and Ya. Yasevichyute, Sov.J.Quantum Electron. 7, 1360(1977).
7. Seilmeier, A., K Spanner, A. Laubereau and W. Kaiser, Optics. Comm. 24, 237 (1978).
8. Campillo, A. J., R. C. Hyer and S. L. Shapiro, to be published.
9. Weisman, R. B. and S. A. Rice, Optics Comm. 19, 28 (1976).
10. Herbst, R. L. and R. L. Byer, Appl. Phys. Lett. 19, 527 (1971).
11. Harris, S. E., Proc. IEEE 57, 2096 (1969).
12. Hobden, M. V. and J. Warner, Phys. Lett 22, 243 (1966).
13. Byer, R. L., PhD dissertation, Microwave Lab Rept. 1711, Stanford University, Stanford, CA, Dec. 1968.

FIGURE CAPTIONS

Fig. 1. Schematic of experimental configuration of traveling wave parametric system used to generate broadly tunable picosecond infrared pulses.

Fig. 2. Observed frequency of the lithium niobate OPA as a function of grating angle. The solid line is that predicted by Eq. 1. α and β are angles of the incident and diffracted beams with respect to the grating normal.

Fig. 3. Calculated small signal normalized gain, define as $\text{Gain}/\Gamma^2L^2 = \text{sinc}^2(\Delta kL/2)$, versus signal frequency of a 1.064 µm pumped 4.5 cm long lithium niobate OPA at θ equal to 44.672° (A), 44.68° (B) and 44.69° (C). Index of refraction dat of Ref. 12 was used in the computations. T = 293°K.

Fig. 4. Calculated normalized small signal gain, Gain/Γ^2L^2, versus signal frequency for several angles α, defined as the angle between k_p and k_s (see insert). k_p is propagated at the degenerate angle, $\theta_{deg.}$, and k_i is oriented to minimize Δk in the computations. The lithium niobate crystal is 4.5 cm in length and T = 293°K.

Fig. 5. Calculated normalized gain versus signal frequency for a 1.064 µm pumped 4.5 cm lithium niobate OPA at T = 293°K. Here the normalized gain is defined by the expression, $\text{Gain}/\sinh^2(\Gamma L) = \Gamma^2L^2 \sinh^2[(\Gamma^2 - \Delta k^2/4)^{1/2}L]/(\sinh^2(\Gamma L))(\Gamma^2 - \Delta k^2/4)L^2$. θ = 44.69° is the approximate operating angle of our traveling wave parmetric oscillator.

Fig. 6. Calculated (solid line) and measured normalized gain versus signal frequency for a 1.064 µm, 4 GW/cm^2 pumped 2 cm lithium niobate OPA at 293°K.

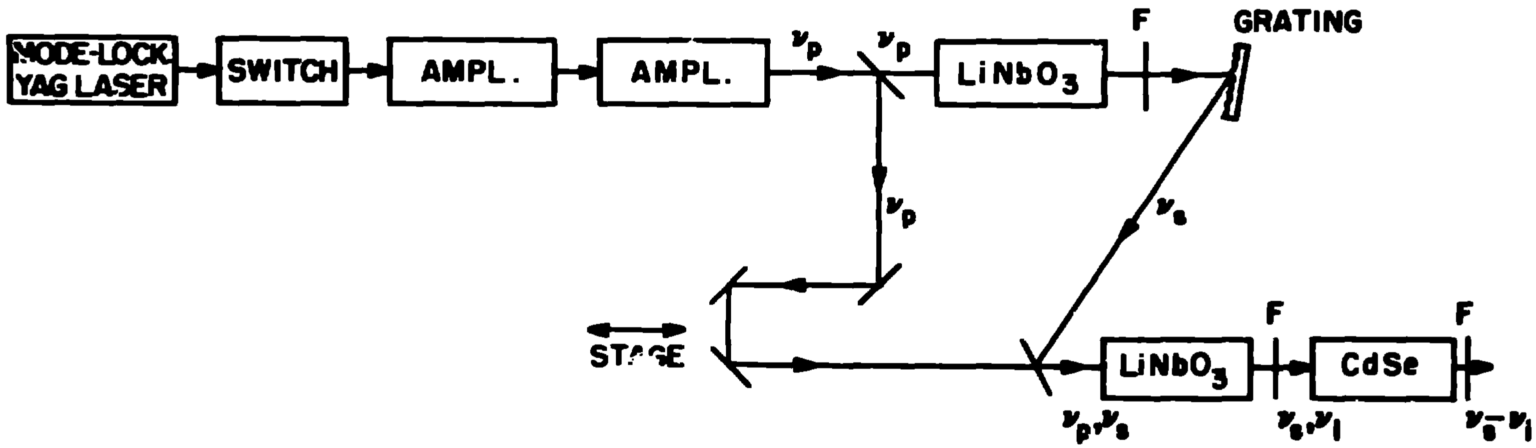
MODE-LOCK YAG LASER
SWITCH
AMPL.
AMPL.
LiNbO3
F
GRATING
STAGE
LiNbO3
F
CdSe
F

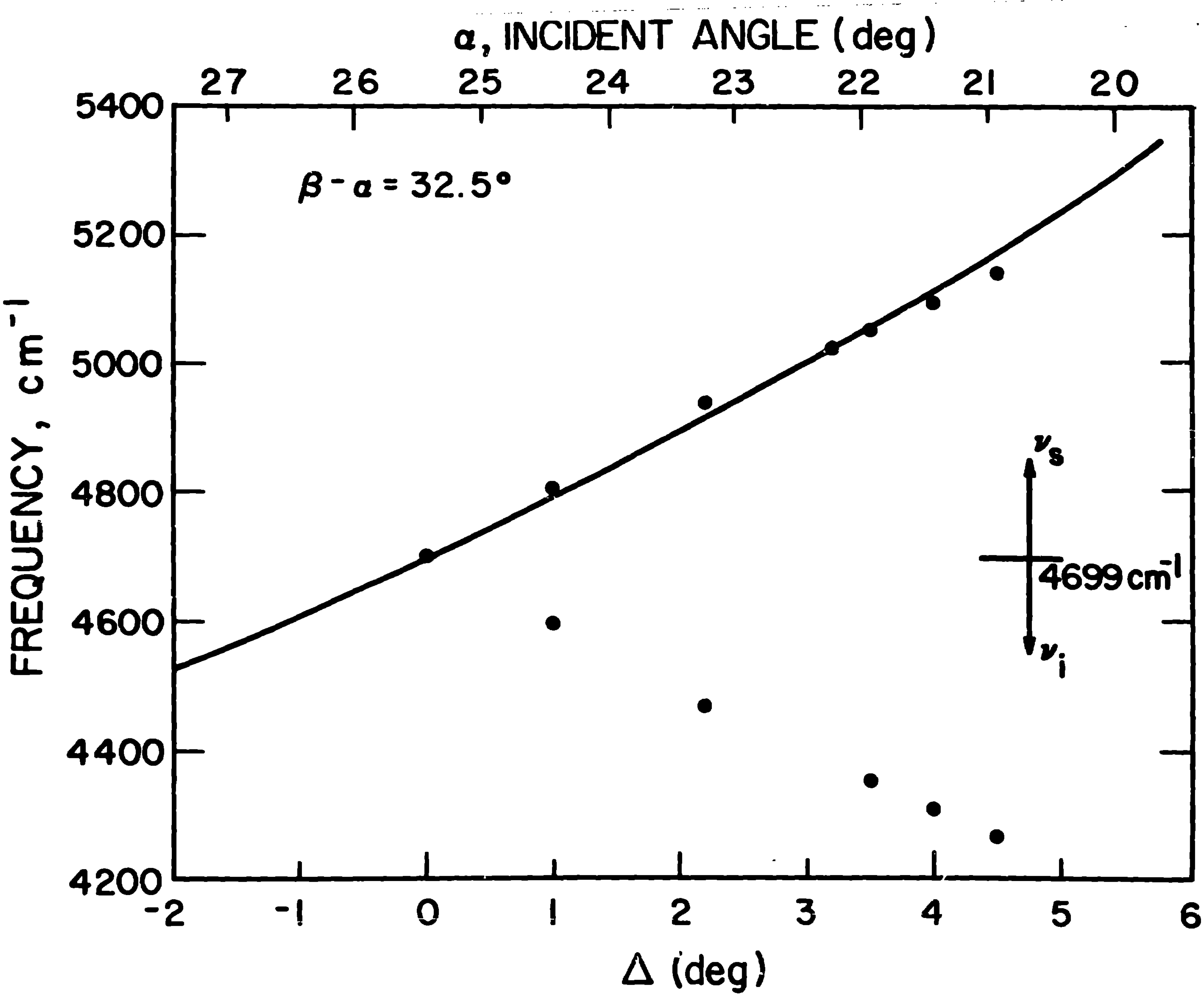

α, INCIDENT ANGLE (deg)
27
26
25
24
23
22
21
20
5400
5200
5000
4800
4600
4400
4200
β - α = 32.5°
FREQUENCY, cm⁻¹
ν_s
4699 cm⁻¹
ν_i
-2
-1
0
1
2
3
4
5
6
Δ (deg)

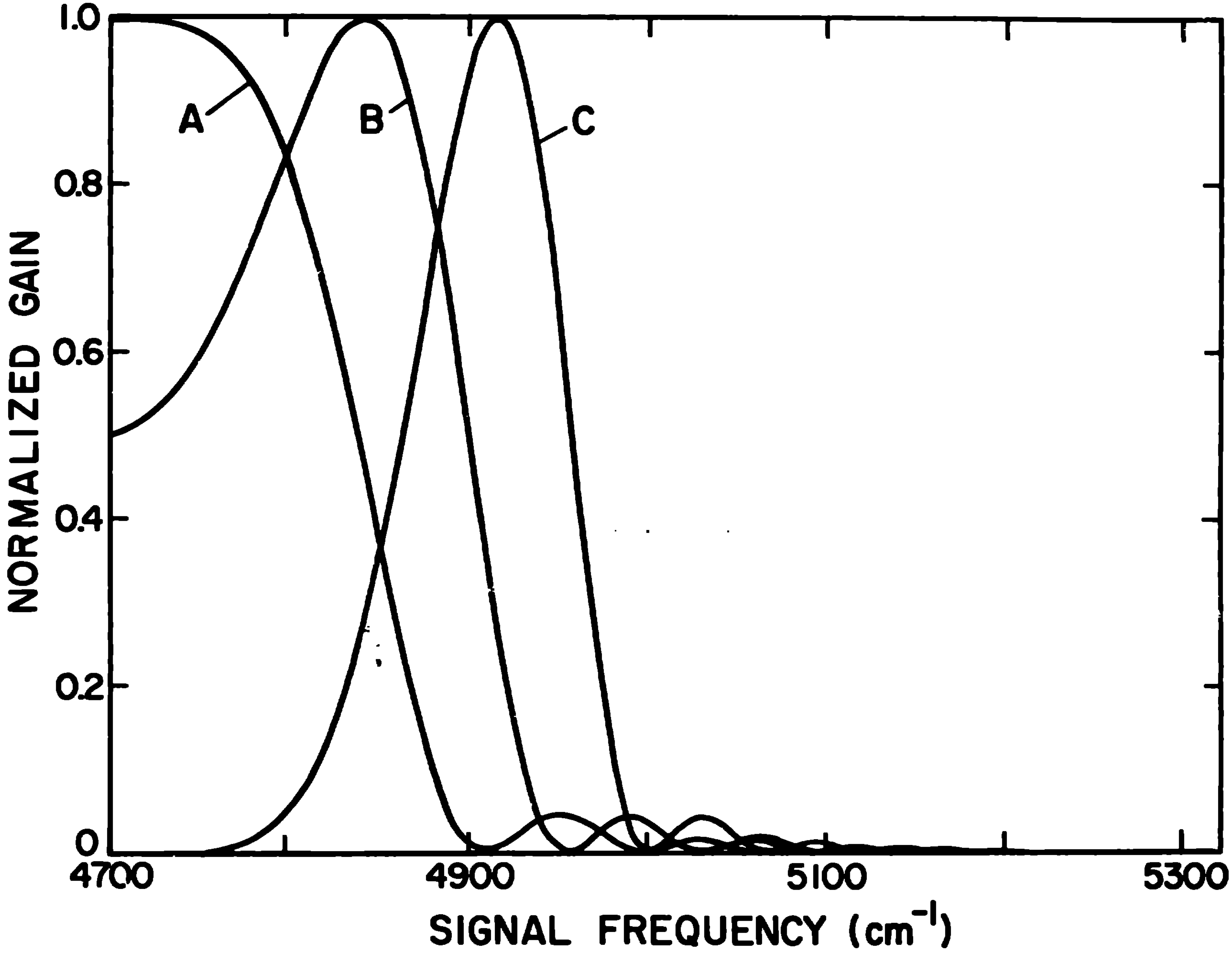

1.0
0.8
0.6
0.4
0.2
0
NORMALIZED GAIN
A
B
C
4700
4900
5100
5300
SIGNAL FREQUENCY (cm^{-1})

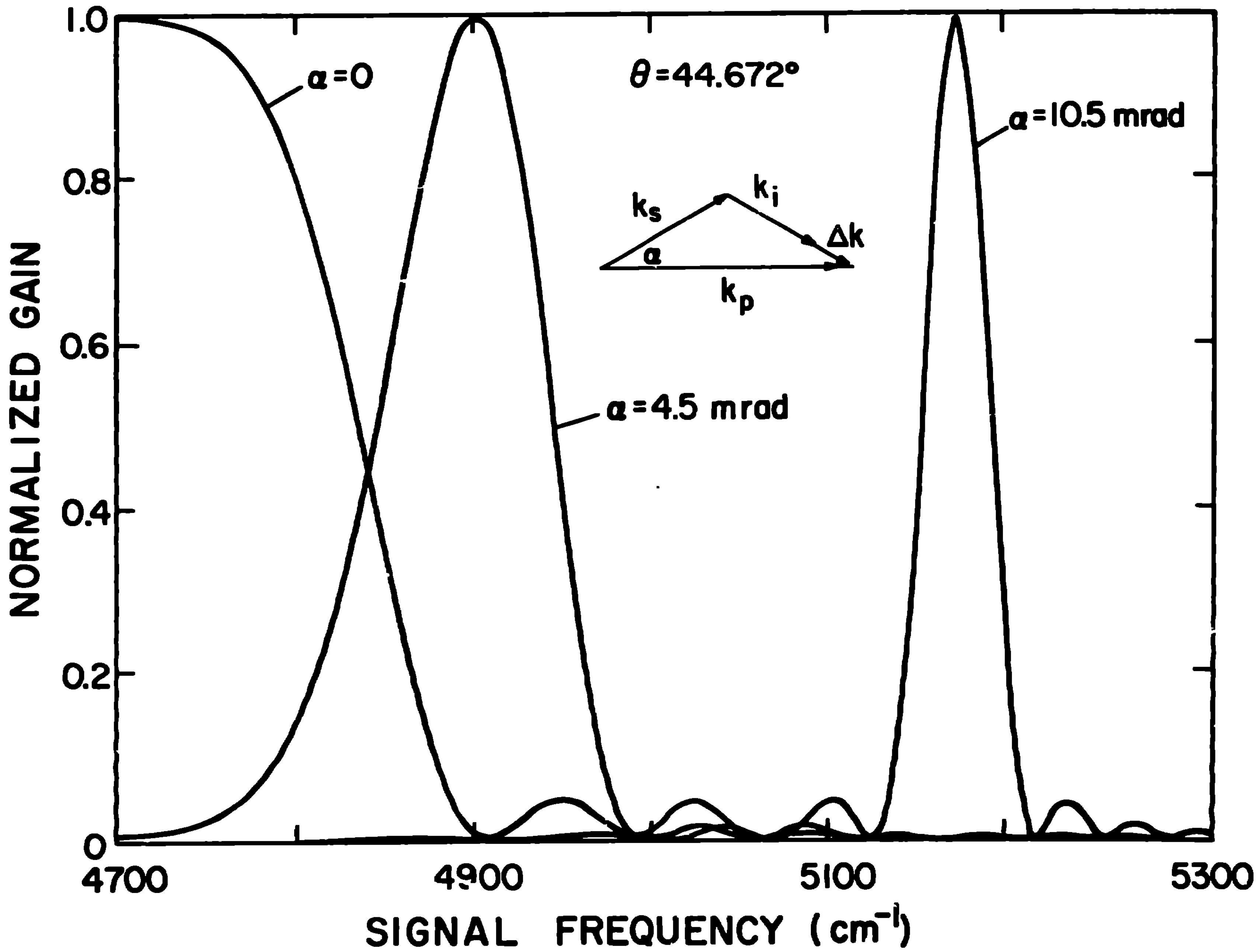

1.0
0.8
0.6
0.4
0.2
0
NORMALIZED GAIN
4700
4900
5100
5300
SIGNAL FREQUENCY (cm⁻¹)
α=0
θ=44.672°
α=10.5 mrad
α=4.5 mrad
k_s
k_i
Δk
α
k_p

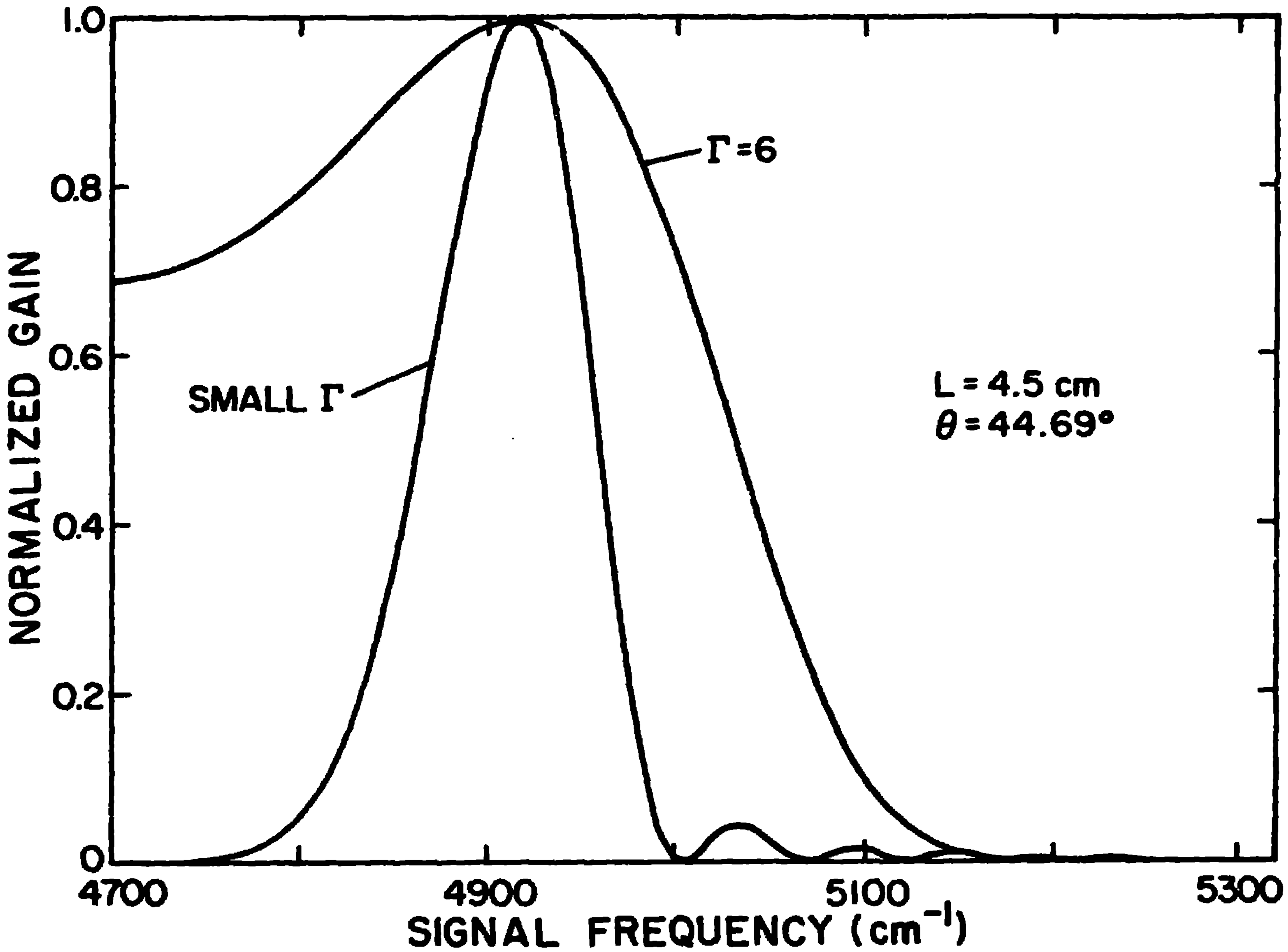
1.0
0.8
0.6
0.4
0.2
0
NORMALIZED GAIN
Γ=6
SMALL Γ
L = 4.5 cm
θ = 44.69°
4700
4900
5100
5300
SIGNAL FREQUENCY (cm⁻¹)

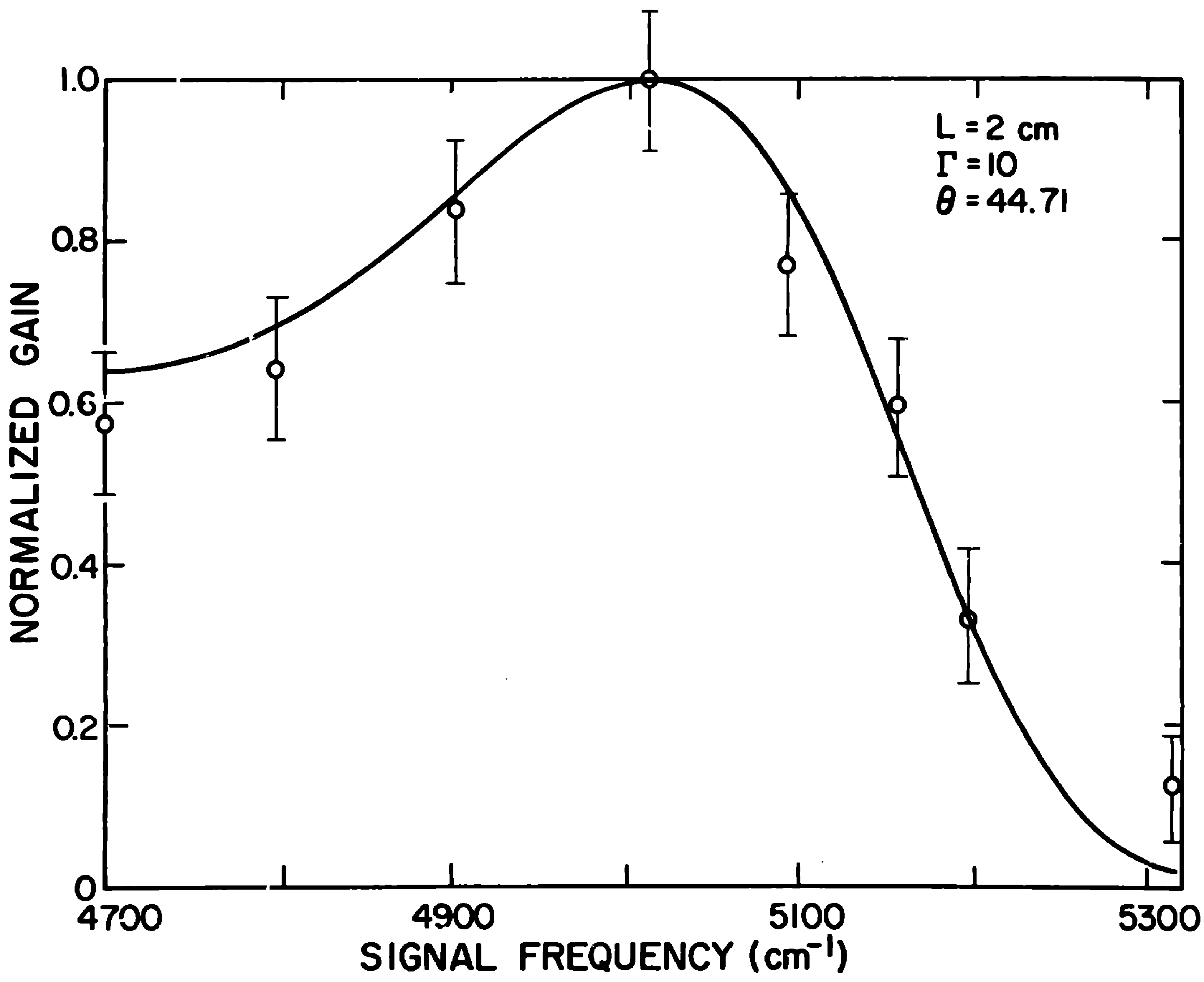
L = 2 cm
Γ = 10
θ = 44.71
NORMALIZED GAIN
1.0
0.8
0.6
0.4
0.2
0
4700
4900
5100
5300
SIGNAL FREQUENCY (cm⁻¹)